Fragmentation Dynamics of Solvent-Clustered Ion Pairs

Regina F. Frey and Jack Simons*

Chemistry Department, University of Utah, Salt Lake City, Utah 84112 *(Received: August 26, 1986)*

Molecular dynamics simulation techniques are used to study the rates of fragmentation and branching ratios of prototype energized ion-pair clusters of the form $NO_2^-:Li^+(H_2O)_n$ (n = 1, 2, ..., 5). Kinetic energy carried away by ejected H_2O molecules, which contributes to the evaporative cooling of the daughter clusters, is found to play a key role in determining the branching ratios. For smaller clusters, geometry-imposed energy-transfer bottlenecks are also seen to strongly affect these branching ratios. The absolute rates of sequential H_2O loss as well as the kinetic energy distributions of the ejected solvent molecules are found to depend upon how the clusters are energized (i.e., whether the energy is deposited via photoabsorption or thermal heating).

I. Introduction

Gas-phase clusters consisting of ions surrounded by small numbers of solvent molecules have been of particular experimental interest recently. There are two basic types of experimental studies being performed on such clusters. One involves the study of equilibrium energetics and structures of the ion clusters;[1-5] the other examines the photodissociation of the cluster into its various possible fragments.[6-9] Most of the experimental work done thus far has been on clusters containing a single ion; little has yet been accomplished, and to our knowledge, nothing has been published on solvent-clustered ion pairs in the gas phase.

In anticipation of future experimental interest and as a spinoff of our own equilibrium Monte Carlo (MC) studies,[10-12] we became interested in studying small hydrate clusters of the prototype ion pair $NO_2^-:Li^+$. Recently, we performed MC studies of the equilibrium geometrical structures and energetics of the hydrate clusters $NO_2^-:Li^+(H_2O)_n$ ($1 \le n \le 28$) and found novel behavior in the solvent-shell geometrical structures as well as evidence for the occurrence of both intimate and solvent-separated ion pairs in larger clusters ($n \ge 25$).[13]

Our decision to use NO_2^- and Li^+ as our prototype ions is rooted in our earlier work on $NO_2^-(H_2O)_n$ and, quite frankly, is related to the availability of reasonable interspecies potential energy functions for $NO_2^-:Li^+(H_2O)_n$.[10-12] We found the high nonspherical NO_2^- anion to display interesting energetic and geometrical effects in its first two hydration shells. We wanted to examine these effects in the ion-pair case, so we chose to work with a spherical cation (Li^+) in order to avoid the introduction of further asymmetry to the hydration potential energy hypersurface. We do not claim that our quantitative results on this *particular* ion-pair cluster are highly accurate; we use rather crude potential energy functions to describe the interspecies interactions. We instead feel that the strength of this work lies in the qualitative features which it uncovers in the ion-pair solvation and fragmentation events. We feel that the $NO_2^-:Li^+(H_2O)_n$ model system contains most of the essential ingredients which are operative in any ion-pair-plus-solvent situation: a range of interspecies interactions ($Li^+:NO_2^- > Li^+:H_2O \approx NO_2^-:H_2O > H_2O:H_2O$), both spherical ($Li^+$) and nonspherical ($NO_2^-$) ions, and multiple branching paths for energized fragmentation (i.e., loss of solvent or ion-pair fragmentation).

In the present paper, we examine *dynamical behavior* of the smaller clusters $NO_2^-:Li^+(H_2O)_n$ ($1 \le n \le 5$) via classical trajectory techniques. We are interested in probing the fragmentation dynamics of the clusters as functions of cluster size and of how the energy is initially deposited into the cluster (e.g., to distinguish between thermally heated clusters and "hot" clusters formed by "photodissociation" of the ion pair). To examine these two distinctly different types of energized clusters, we performed two sets of molecular dynamics (MD) calculations using cluster sizes ranging from 1 to 5 water molecules. Although we may, in further work, extend this study to larger clusters ($n > 5$), we found sufficiently interesting behavior in these smaller clusters to warrant communication of our results in their present form.

A. Thermally Hot Clusters. In our first simulations, involving what we refer to as *thermally hot clusters*, we equipartition the total energy E_{tot} among all of the cluster's degrees of freedom. (We do not consider the internal vibrational degrees of freedom of the molecules (see below).) In all such studies, we chose E_{tot} such that the energy per degree of freedom is independent of cluster size and is equal to approximately 1000 cm^{-1}. Such average energies are much larger than have been utilized in experimental work to date on solvent-clustered single ions. We decided to examine this range of average energies first because we wanted to explore the cooperation between ion–ion fragmentation and solvent molecule loss. Moreover, we wanted to initially consider the shorter time dynamics of our clusters within which the numerical integration algorithms we used should remain stable. The study of longer time (i.e., microsecond) dynamics is a much more formidable task.

B. Photodissociated Clusters. In the second type of simulations, involving what we refer to as *photodissociated clusters*, we again distribute an equal (but smaller) amount of energy E_{small} among each of the cluster's degrees of freedom; we then add to the interion relative kinetic energy an amount of energy ΔE designed to simulate an impulsive dissociation of the ion pair. The total energy $E_{small} + \Delta E$ for a given cluster size is arranged to equal the total energy E_{tot} used in the thermally hot cluster study for the same cluster size. In this way, we can then examine effects resulting from how the energy is initially deposited into the cluster at fixed energy per degree of freedom ($\sim$1000 cm^{-1}).

C. Monitoring Trajectories. We are interested in the transfer of energy among the cluster's degrees of freedom and the ultimate fate of this energy for both the thermally hot and the photodissociated clusters. To monitor such quantities, we calculate the lifetimes for the sequential loss of water molecules and for ion–ion dissociation as functions of cluster size and initial energy. We also evaluate the branching ratios for the production of various fragment clusters.

We find that the kinetic energy carried away by ejected solvent molecules plays a key role in the subsequent fragmentation behavior of the surviving daughter cluster. The distributions of such

(1) Kebarle, P. *Annu. Rev. Phys. Chem.* **1977**, *28*, 445.
(2) Sunner, J.; Kebarle, P. *J. Phys. Chem.* **1981**, *85*, 327.
(3) Keesee, R. G.; Lee, N.; Castleman, Jr., A. W. *J. Am. Chem. Soc.* **1979**, *101*, 2599.
(4) Lee, N.; Keesee, R. G.; Castleman, Jr., A. W. *J. Chem. Phys.* **1980**, *72*, 1089.
(5) Banic, C. M.; Iribane, J. V. *J. Chem. Phys.* **1985**, *83*, 6432.
(6) Hunton, D. E.; Hofmann, M.; Lindeman, T. G.; Albertoni, C. R.; Castleman, Jr., A. W. *J. Chem. Phys.* **1985**, *82*, 2884.
(7) Echt, O.; Dao, P. D.; Morgan, S.; Castleman, Jr., A. W. *J. Chem. Phys.* **1985**, *82*, 4076.
(8) Johnson, M. A.; Alexander, M. L.; Lineberger, W. C. *Chem. Phys. Lett.* **1984**, *112*, 285.
(9) Alexander, M. L.; Johnson, M. A.; Lineberger, W. C. *J. Chem. Phys.* **1985**, *82*, 5288.
(10) Banerjee, A.; Simons, J. *J. Chem. Phys.* **1979**, *68*, 415.
(11) Banerjee, A.; Shepard, R.; Simons, J. *J. Chem. Phys.* **1980**, *73*, 1814.
(12) Banerjee, A.; Simons, J. *J. Am. Chem. Soc.* **1981**, *103*, 2180.
(13) Banerjee, A.; Quigley, A.; Frey, R. F.; Johnson, D.; Simons, J., submitted for publication to *J. Am. Chem. Soc.*

0022-3654/87/2091-2818$01.50/0

kinetic energies as functions of cluster size and energy deposition are also examined.

In section II, we describe the interparticle potentials used in the classical trajectory simulations employed in this work; section III describes some of the details of our classical trajectory method. We discuss our findings in section IV, and section V contains our concluding remarks.

II. NO_2^-:$Li^+(H_2O)_n$ Potentials

The functional form of the potential energy for the cluster NO_2^-:$Li^+(H_2O)_n$ is taken to be the same as we used in our earlier Monte Carlo work and is discussed in detail in ref 13. Briefly, we first assume that the NO_2^- and H_2O species are rigid bodies. The bond lengths and angles of NO_2^- and H_2O are frozen at their isolated-species equilibrium values: $R_{NO} = 1.26$ Å, $\theta_{ONO} = 117°$ and $R_{OH} = 0.95$ Å, $\theta = 111.3°$, respectively. At the internal energies used in our simulations, the NO_2^- bending (800 cm^{-1}) and stretching motions (1280, 1320 cm^{-1}) and the H_2O bending (1300 cm^{-1}) are likely to become appreciably excited. Although the neglect of these degrees of freedom further limits the accuracy of our findings, we believe that the general features of our results will be unchanged were we to include them.

The total interspecies potential energy is represented as a sum of pair potentials for NO_2^-:H_2O, Li^+:H_2O, NO_2^-:Li^+, and H_2O:H_2O. A series of studies on H_2O by Morse and Rice[14,15] and by Clementi et al.[16-18] have shown the importance of including many-body terms in the H_2O:H_2O potentials. Clementi et al. have shown that many-body interactions can comprise as much as 15% of the internal energy.[17] Nevertheless, we chose to include only pairwise additive potentials both to keep our computational expense within limits and because we feel that 15% errors are not going to affect the qualitative features which we are trying to identify in this work.

The pair potentials for NO_2^-:H_2O, NO_2^-:Li^+, and Li^+:H_2O were obtained (ref 11, 13, and 19) as fits to the restricted Hartree–Fock (HF) interaction potentials of the ground electronic states of the respective pairs. The potential used for H_2O:H_2O is Clementi's fit of his configuration interaction (CI) potential for the ground state of the H_2O:H_2O dimer.[20] The functional form of all of the interspecies potentials is given as

$$V = \sum_{i,j} a_{ij} \frac{1}{r_{ij}} + \sum_{i,j} \exp[c_{ij} r_{ij}] \qquad (1)$$

where I and J represent index atoms on separate molecules; the values of the a, b, and c parameters are given in ref 11, 13, 19, and 20.

III. Classical Trajectory Method

A. Initial Positions and Velocities. To simulate the dynamics of the clusters, we examined the time evolution of 50–100 trajectories for each cluster size for a duration of 20 ps using time steps of approximately 10^{-15} s. To obtain a distribution of initial configurations of the molecules appropriate to an equilibrium ensemble at temperature T, we first performed a Metropolis MC calculation[21] on each cluster at a temperature of 300 K and used the resulting MC spatial distributions from which to choose initial coordinates. To obtain the initial velocity for each degree of freedom, we placed the same amount (1000 cm^{-1} for the thermally hot clusters and 300 cm^{-1} for the photodissociated clusters) of total energy (kinetic plus potential) into each degree of freedom (i.e., we equipartitioned the total energy) with random directions of the velocities. We then began the trajectory and allowed it to proceed for 20–30 times steps of 1.7×10^{-15} s each before we began to collect data for the next $\sim 10^4$ time steps. We did this "trajectory aging" to establish stability of the numerical integration algorithm and to allow for full equipartitioning of the energy before we began to collect data. This process allows the positions and momenta of the ions and solvent species to "adjust" to the 300 or 1000 cm^{-1} of energy per degree of freedom. In those cases where we simulate the photodissociated clusters, after we thus "aged" the trajectory, we then placed an additional amount of energy ΔE into the translational degree of freedom of the ion pair in a manner such that total angular momentum is conserved (see section I for a definition of ΔE).

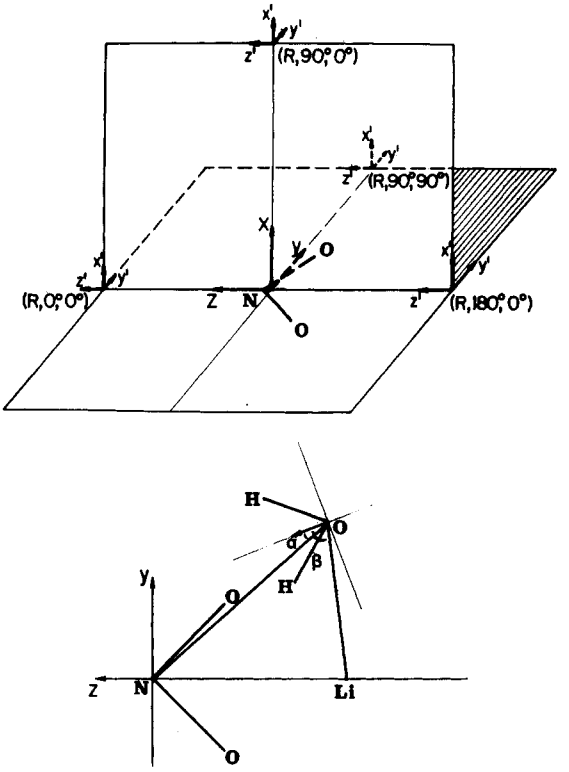

Figure 1. Coordinate system for describing the $NO_2^-Li^+(H_2O)_n$ cluster. (a, top) (R,θ,ϕ) are used to describe the positions of the Li^+ atom or of center-of-mass of the water molecule relative to the center-of-mass of the NO_2^- ion. (b, bottom) The angles α and β describe the orientation of the water's dipole vector.

B. Equations of Motion. Newton's equations of motion were used to describe the interspecies translational degrees of freedom of the system. For the rotational degrees of freedom of NO_2^- and H_2O, Euler's equations of motion were expressed in terms of quaternions[22,23] in order to remove the singularities at $\theta = 0$ and π that are present when one used Euler angles. The Appendix contains more details on the resultant quaternion equations of motion.

All integrations of the equations of motion were performed using a fourth-order Adams–Moulton predictor–corrector method preceded by an Euler's method integration for the first four time steps to initialize the Adams–Moulton integrator. The time step of 1.7×10^{-15} s was found to conserve energy to within 2% for the duration of the trajectory.

C. Monitoring. We monitored both structural and kinetic information as the trajectories evolved. To acquire time-averaged structural information, the following geometrical parameters were histogrammed at uniform time steps (the coordinates R, θ, ϕ, α, and β are defined in Figure 1): (1) relative distances between pairs of atoms on different molecules, (2) the angles (α, β) which give the direction the water molecules are facing relative to the

(14) Morse, M. D.; Rice, S. A. *J. Chem. Phys.* **1982**, *76*, 650.
(15) Morse, M. D.; Rice, S. A. *J. Chem. Phys.* **1981**, *74*, 6514.
(16) Clementi, E.; Corongiu, G. *Int. J. Quantum Chem.* **1983**, *10*, 31.
(17) Detrich, J.; Corongiu, G.; Clementi, E. *Chem. Phys. Lett.* **1984**, *112*, 426.
(18) Wojcik, M.; Clementi, E. *J. Chem. Phys.* **1986**, *84*, 5970.
(19) Clementi, E.; Popkie, H. *J. Chem. Phys.* **1972**, *57*, 1077.
(20) Matsuoka, O.; Clementi, E.; Yoshimine, M. *J. Chem. Phys.* **1975**, *64*, 1351.
(21) Metropolis, N.; Metropolis, A. W.; Rosenbluth, M. N.; Teller, A. H.; Teller, E. *J. Chem. Phys.* **1953**, *21*, 1087.
(22) Evans, D. J. *Mol. Phys.* **1977**, *34*, 317.
(23) Goldstein, H. *Classical Mechanics*; Addison-Wesley: CA, 1980; p 153.

TABLE I: Energy Contents and Requirements for $NO_2^-:Li^+(H_2O)_n$

cluster size (n)	total amount of energy,[b] cm^{-1}	energy needed to dissociate $NO_2^-:Li^+$ ion pair,[a] cm^{-1}	energy needed to lose all waters,[a] cm^{-1}
1	15000	45000	12000
2	21000	34000	20000
3	27000	41000	28000
4	33000	39000	32000
5	39000	38000	37000

[a] Determined from Monte Carlo calculations (ref 13). [b] Relative to the absolute minimum in the cluster potential energy surface.

TABLE II: Bond Energies for H_2O Molecules

species	bond energies from MC, cm^{-1}
$NO_2^-:Li^+(H_2O) \rightarrow NO_2^-:Li^+ + H_2O$	12000
$NO_2^-:Li^+(H_2O)_2 \rightarrow NO_2^-:Li^+(H_2O) + H_2O$	8300
$NO_2^-:Li^+(H_2O)_3 \rightarrow NO_2^-:Li^+(H_2O)_2 + H_2O$	7400
$NO_2^-:Li^+(H_2O)_4 \rightarrow NO_2^-:Li^+(H_2O)_3 + H_2O$	4500
$NO_2^-:Li^+(H_2O)_5 \rightarrow NO_2^-:Li^+(H_2O)_4 + H_2O$	4800

NO_2^- and Li^+ ions, and (3) the coordinates (R,θ,ϕ) of the Li^+ ion relative to the NO_2^- ion.

In addition to these structural data, we also monitored the branching ratios and the sequential dissociation rates of the water molecules leaving the cluster.[24] We fit the water-loss decay profiles (see, for example, Figure 2) to a single- or double-exponential functions of the form

$$Ae^{-k_F t} + Be^{-k_S t} + C \qquad (2)$$

where k_F and k_S are referred to as "fast" and "slow" decay rate constants and the ratio of A and B measures the fraction of quickly and slowly decaying trajectories. The value of C is a measure of the number of trajectories which do not decay within the 20 ps of our numerical experiment.

Finally, we monitored the distribution of kinetic energy (translational and rotational) carried away by the ejected solvent molecules in an attempt to examine the effects of "evaporative cooling" of the daughter cluster on the rate of subsequent solvent loss. We were interested in exploring the extent to which these kinetic energy distributions followed "statistical" patterns which seem to arise in recent work in other clusters.[25]

IV. Results

A. Energetic Considerations. As stated previously, we performed two types of simulations. The first involves the thermally hot clusters; here all of the active cluster degrees of freedom have the same amount of energy initially. For example, we examined the behavior of n = 1–5 clusters which have 1000 cm^{-1} of total energy per degree of freedom initially. The total amount of energy (relative to the absolute minimum in the cluster's potential energy surface) for each size cluster is given in Table I as are the energies needed to dissociate the ion pair and to remove all solvent molecules from the ion pair.

Because we operate at energies below the dissociation energies of the chemical bonds in H_2O and NO_2^-, we need only concern ourselves with fragmentation of the interspecies cluster modes. From our previous Monte Carlo calculations,[13] we determined the amount of energy needed to dissociate the clusters into separated but solvated ions for each size cluster (Table I), as well as the energies required to sequentially and adiabatically remove water molecules from the ion-pair clusters (Table II). Examining the total amount of energy available in each cluster, we see that all of the clusters have enough energy to lose *all* of their water molecules. However, only the 5-water cluster has enough energy to dissociate the ion pair (keeping the water molecules bound to the ions). Let us now move on to examine our findings keeping in mind the above energetic restrictions. In particular, it will be interesting to note whether all solvent molecules are actually lost and at what rates. It will also be interesting to see whether the n = 5 cluster actually dissociates into separated ions at any appreciable rate and whether or not the behavior patterns of the isoenergetic thermally hot and photodissociated clusters are similar.

B. Dissociation Rates and Branching Ratios. Tables III and IV show, for the thermally hot and photodissociated cases, the sequential "fast" and "slow" water dissociation lifetimes ($\tau_{F,S} = k_{F,S}^{-1}$), the fraction of the trajectories following the fast and slow

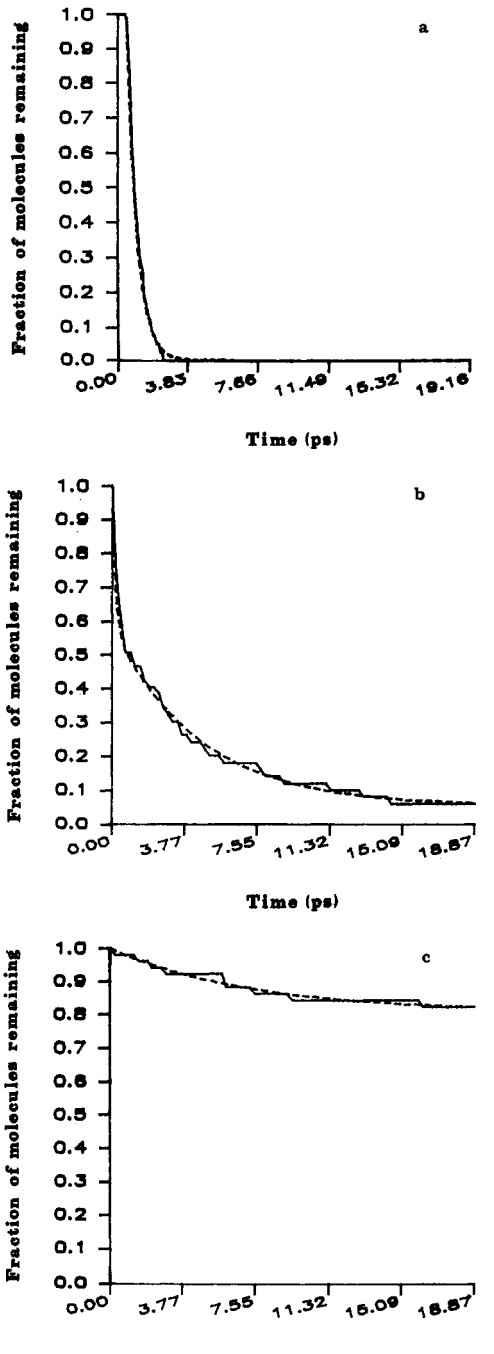

Figure 2. Exponential fits of the sequential water loss in the thermally hot 4-water cluster for ejection of the first, second, and third waters, respectively.

(24) To determine when a water molecule has ejected from the cluster, we first monitor the distance the water molecule is from the cluster. The molecule is considered as having left if the distance from each ion is greater than the distance corresponding to 92% of the dissociation energy of the pair potential of water with that ion. For $NO_2^-:H_2O$ and $Li^+:H_2O$, these distances are 12.8 and 7.9 Å, respectively. If the position of the water molecule meets this first criterion, then the direction the water molecule is moving in relation to the cluster is examined. The direction of the velocity for the water must be in the opposite direction of the velocities for both of the ions. When both of these criteria have been met, then the water molecule is viewed as having left the cluster.

(25) Engelking, P. C., personal communication.

TABLE III: Sequential H_2O-Loss Dynamics for Thermally Hot Clusters

no. of water molecules in cluster	nth H_2O ejected	results of exponential fits to dissociation plots[a]					resultant branching ratios for production of $NO_2^-:Li^+(H_2O)_m$	
		A	B	C	k_F^{-1}, ps	k_S^{-1}, ps	m	%
5	1	0.96	0.0	0.04	0.6		5	4
	2	0.52	0.26	0.22	0.5	3.7	4	21
	3	0.30	0.24	0.46	1.5	7.5	3	35
	4	0.10	0.26	0.64	1.7	30.0	2	26
	5	0.0	0.0	1.0			1	14
							0	0
4	1	1.0	0.0	0.0	0.6		4	0
	2	0.41	0.53	0.06	0.2	4.6	3	6
	3	0.20	0.0	0.80	7.0		2	75
	4	0.0	0.0	1.0			1	18
							0	0
3	1	0.07	0.86	0.07	0.2	1.7	3	7
	2	0.05	0.70	0.25	0.2	1.6	2	23
	3	0.0	0.0	1.0			1	70
							0	0
2	1	0.93	0.0	0.07	3.9		2	7
	2	0.0	0.0	1.0			1	93
							0	0
1	1	0.47	0.0	0.53	8.4		1	53
							0	47

[a] The exponential equation we fit to is $N(\tau) = Ae^{-k_F(\tau)} + Be^{-k_S(\tau)} + C$ where the dissociation lifetime for the waters departing is $\tau_{F,S} = k_{F,S}^{-1}$.

TABLE IV: Sequential H_2O-Loss Dynamics for Photodissociated Clusters

no. of water molecules in cluster	nth H_2O ejected	results of exponential fits to dissociation plots[a]					resultant branching ratios for production of $NO_2:Li^+(H_2O)_m$	
		A	B	C	k_F^{-1}, ps	k_S^{-1}, ps	m	%
5	1	1.0	0.0	0.0	0.7		5	0
	2	0.71	0.29	0.0	1.1	6.6	4	0
	3	0.17	0.78	0.05	0.3	1.4	3	5
	4	0.0	0.0	1.0			2	95
	5	0.0	0.0	1.0			1	0
							0	0
4	1	0.98	0.0	0.02	0.6		4	2
	2	0.54	0.0	0.46	4.5		3	45
	3	0.0	0.0	1.0			2	53
	4	0.0	0.0	1.0			1	0
							0	0
3	1	1.0	0.0	0.0	3.5		3	0
	2	0.07	0.0	0.93	3.2		2	93
	3	0.0	0.0	1.0			1	7
							0	0
2	1	0.31	0.0	0.69	14.0		2	70
	2	0.0	0.0	1.0			1	30
							0	0
1	1	0.0	0.0	1.0			1	100
							0	0

[a] The exponential equation we fit to is $N(\tau) = Ae^{-k_F(\tau)} + Be^{-k_S(\tau)} + C$ where the dissociation lifetime for the waters departing is $\tau_{F,S} = k_{F,S}^{-1}$.

paths (A and B in eq 2), the fraction of trajectories which do not undergo that H_2O loss (C in eq 2), and the resultant branching ratios.

1. 4-Water Cluster Dynamics. To illustrate the interpretation of our results, we take as an example the *thermally hot 4-water cluster*. Figure 2 shows the decay plots for the sequential loss of the water molecules, and Figure 3 shows the corresponding histograms of the relative kinetic energy taken away by the departing water molecules.[26] As can be seen from Figure 2a and Table III's A, B, and C values, all trajectories lose the *first* water molecule within a lifetime of ~0.6 ps. The total kinetic energy histogram (Figure 3a) shows that this first water takes with it, on average, a kinetic energy of ~4300 cm^{-1} when it departs. Figure 2b relates to the sequential loss of the *second* water molecule from which it can be seen that ~90% of the clusters also lose a second water, those that do not remain as NO_2^-:$Li^+(H_2O)_3$ for at least the 20-ps duration of our "experiment". Approximately 40% of these second water molecules exit quickly ($\tau \sim 0.2$ ps), and ~53% leave with a longer lifetime ($\tau \sim 4.6$ ps). According to Figure 3b, the second water molecules take away ~3200 cm^{-1} of kinetic energy when they depart. Figure 2c shows that only 20% of the clusters which lost two waters lose their *third* water. The lifetime for loss of the third water molecule is ~7.0 ps, and its average kinetic energy upon departure is ~2000 cm^{-1} (Figure 3c). Taking into account the amount of energy needed to eject the various water molecules and the (average) amount of kinetic energy[27] carried away by these water molecules,

(26) The detailed structures which appear in these histograms are thought to be largely artifacts of the small samples (50–100 trajectories) utilized. We examined these histograms for sample sizes ranging from 50 to 500 trajectories and found the detailed structures to be largely irreproducible, although the general "shapes" (e.g., average energy and the width of the distribution) were reproducible.

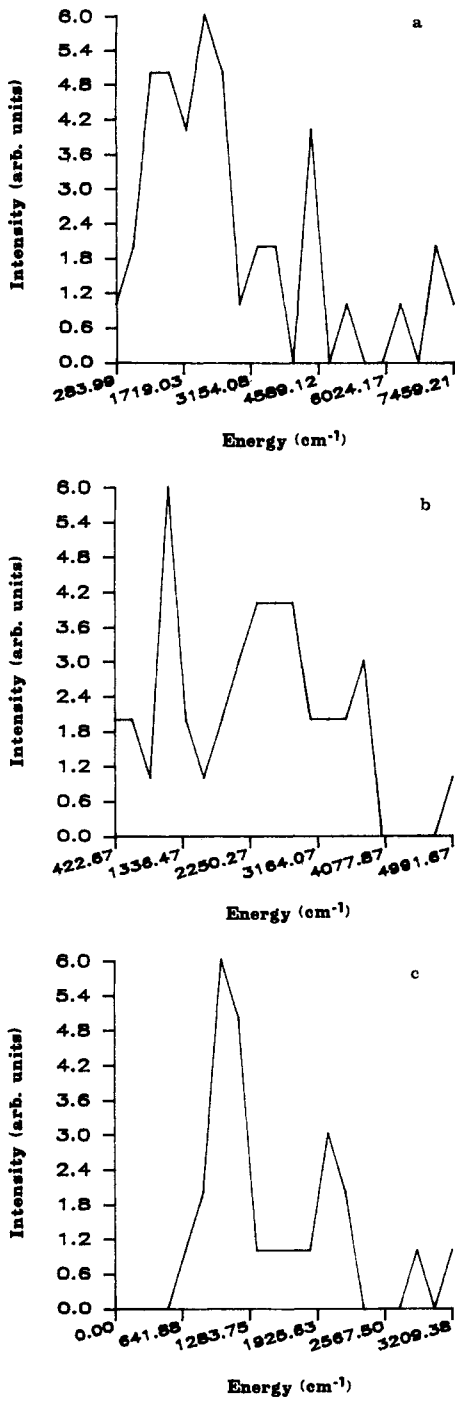

Figure 3. Total kinetic energy histograms corresponding to ejection of the first, second, and third waters, respectively, from the thermally hot 4-water cluster.

it can be seen from Table V that once the 4-water cluster (which started with 33 000 cm^{-1} of internal energy) has lost three water molecules, it has, on average, no more than 3300 cm^{-1} of energy remaining in the cluster's degrees of freedom. To eject the last water from the cluster takes ~12 000 cm^{-1}; hence, there is not enough energy left in the cluster to eject the last water, as is evidenced in the results of Table III. If we had ignored the *kinetic* energy carried away by those water molecules that are ejected, we could not have explained the observation that the 4-water cluster loses only three of its solvent molecules. Thus, kinetic energy disposal is crucial to our understanding.

Let us now compare these observations with the corresponding results on the *photodissociated 4-water cluster*. Figure 4 contains

(27) Note that the ejected H_2O molecules carry away appreciable rotational kinetic energy in addition to their translational energy.

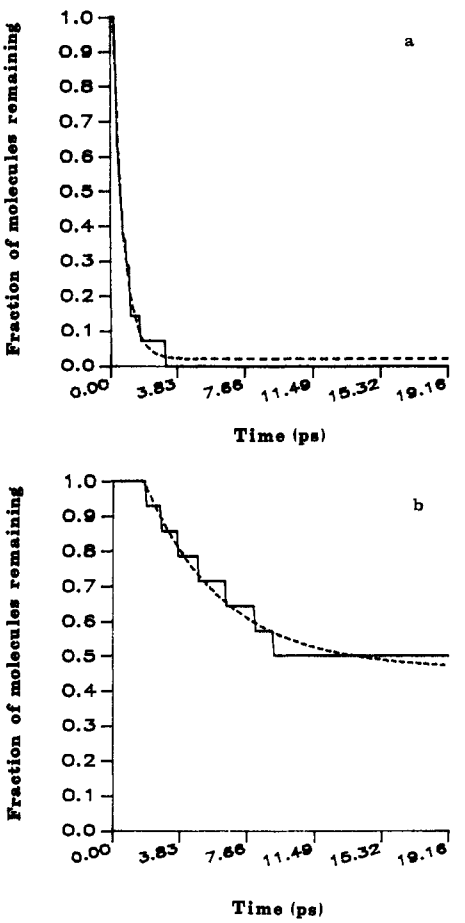

Figure 4. Exponential fits of the sequential water loss in the photodissociated 4-water cluster for ejection of the first and second waters, respectively.

the decay plots for the sequential loss of water molecules, and Figure 5 shows the corresponding total kinetic energy histograms. As seen from Figure 4a and Table IV, essentially all of the trajectories lose the *first* water molecule. The lifetime for the loss of the first water is ~0.6 ps, and the average kinetic energy carried away by this water is ~9900 cm^{-1} (Figure 5a and Table V). Although the lifetime is approximately the same as for the corresponding thermally hot cluster, this first water molecule departs with a much greater average kinetic energy than in the thermally hot cluster. Approximately 54% of the clusters which lost the first water also lose the *second* water molecule. The lifetime for the second water loss is ~4.5 ps, the same as the corresponding slow lifetime of the thermally hot cluster. The total kinetic energy carried away by this water is ~1400 cm^{-1} (Figure 5b and Table V). Once the 4-water cluster (which began with a total energy of 33 000 cm^{-1}) has lost two waters, there is approximately 9800 cm^{-1} of energy remaining. This is enough energy to eject the third water, but not enough to eject both the third and fourth waters from the cluster. As Table IV indicates, the third water molecule is *not* ejected within 20 ps even though there is 9800 cm^{-1} of energy remaining.

2. Overview of Other Clusters. Having described in detail several results for the two types of 4-water clusters, we now return to Tables III–V to overview our results on the other clusters. As stated previously, Tables III and IV list the water-loss lifetimes, the fraction of trajectories having those lifetimes, and the resultant branching ratios, while Table V contains the amount of energy needed to eject the water molecules and the average kinetic energy each water molecule carries away with it.

a. Branching Ratios. As can be seen from Table V, there is enough total energy initially to eject all of the waters from any size cluster if the ejected waters were to carry away no excess (i.e., translational and rotational kinetic) energy. However, once we take into account the (average) kinetic energy taken away by the water molecules which are ejected, a different picture emerges.

TABLE V: Average Kinetic Energy of Escaped H_2O Molecules

no. of water molecules in cluster (total energy content, cm^{-1})	*n*th water ejected	energy needed to eject *n*th water, cm^{-1}	kinetic energy of *n*th water for thermally hot cluster, cm^{-1}		kinetic energy of *n*th water for photodissociated cluster, cm^{-1}	
			total	translational	total	translational
5 (39 000 cm^{-1})	1	4800	2500	2500	2600	1800
	2	4500	5000	3000	3800	3400
	3	7400	1800	1800	1400	1400
	4	8300	1200	1200		
	5	12000				
4 (33 000 cm^{-1})	1	4500	4300	4100	9900	9800
	2	7400	3200	2700	1400	600
	3	8300	2000	900		
	4	12000				
3 (27 000 cm^{-1})	1	7400	2100	1000	2100	1900
	2	8300	1800	1400	1300	1300
	3	12000				
2 (21 000 cm^{-1})	1	8300	1400	1300	4600	4500
	2	12000				
1 (15 000 cm^{-1})	1	12000	900	700		

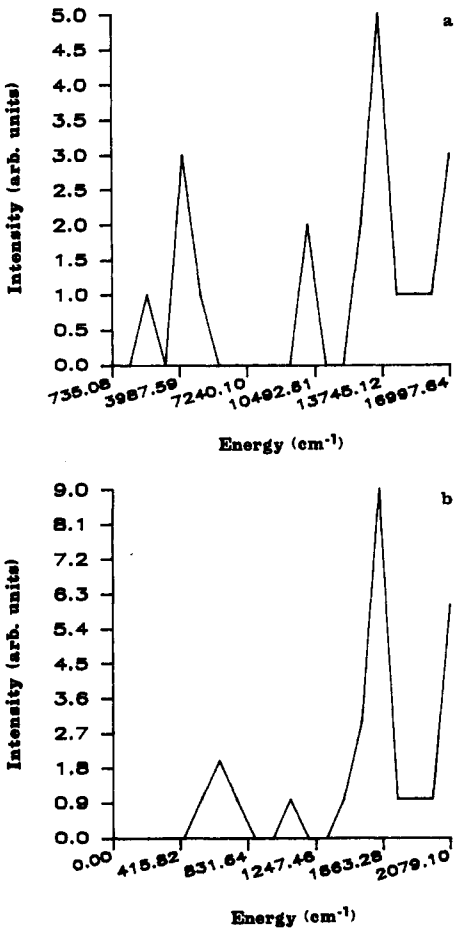

Figure 5. Total kinetic energy histograms corresponding to ejection of the first and second waters, respectively, from the photodissociated 4-water cluster.

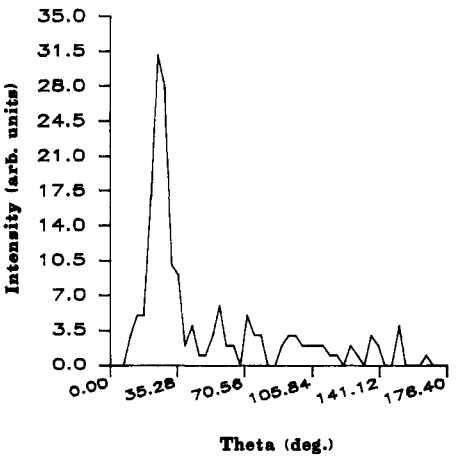

Figure 6. Angular histogram of the water spatial distribution in the photodissociated 1-water cluster.

For example, all of the thermally hot clusters except $n = 1$ do not have enough energy remaining to eject their last water molecule once these kinetic energy effects are taken into consideration.

The branching ratios shown in Table III confirm the prediction that no such thermally hot clusters should lose their last solvent molecule. For the photodissociated clusters, consideration of the average kinetic energy loss leads to the same prediction—that all clusters should lose all but one solvent molecule. However, for the $n = 4$ and $n = 5$ photodissociated clusters, even the next-to-last water molecule remains bound (see Table IV) during our 20-ps numerical experiment even though there exists (on the average) enough internal energy to eject this water. Clearly, the *distributions* of kinetic energy release, not merely the averages, must be considered in order to fully interpret the branching ratios (Tables III and IV) obtained for the thermally hot and photodissociated clusters. Nevertheless, the fact is that both binding energy and kinetic energy release are essential ingredients in determining the branching ratios of such ion-pair clusters.

In comparing the branching ratio patterns between the thermally hot and corresponding photodissociated clusters, one notices significant differences, some of which were quite surprising to us. The first, and most surprising, difference arises in the smaller photodissociated (n = 1,2) clusters where 100% of the $n = 1$ clusters and 70% of the $n = 2$ clusters do not eject even their first solvent molecule within 20 ps, although the corresponding thermally hot clusters eject their first water molecule 47% and 93% of the time within 20 ps. A similar surprise appears for the $n = 3$ clusters once the first solvent molecule is ejected. For the $n = 3$ photodissociated cluster, 93% of the clusters which have ejected their first water do *not* eject the second; for the $n = 3$ thermally hot cluster 70% do eject their second solvent molecule. Quite frankly, we were surprised to find that the smaller photodissociated clusters, which we viewed in terms of an extremely vibrationally hot NO_2^-:Li^+ species with a few weakly attached H_2O molecules, are not able to "shake" off their solvents whereas the thermally hot species are.

In our attempt to understand this puzzling behavior, we examined, via histogram techniques, the spatial distributions of the solvent molecules relative to the NO_2^-:Li^+ moiety for the thermally hot and photodissociated cases. We observed that for the smaller photodissociated clusters the solvent molecules preferentially

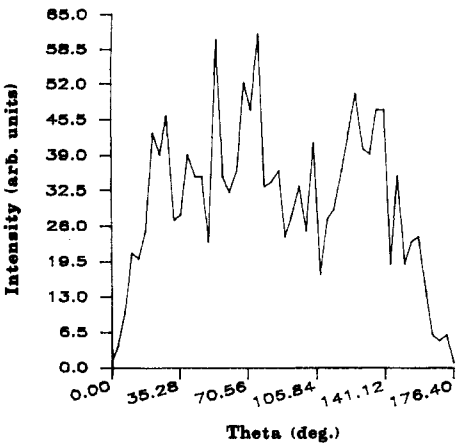

Figure 7. Angular histogram of the water spatial distribution in the thermally hot 1-water cluster.

occupy regions of space not along the NO_2^-:Li^+ interionic axis (e.g., see Figure 6). Recall that these solvent molecules initially possess only 300 cm^{-1} of motional energy per degree of freedom; most of the energy initially resides in the NO_2^-:Li^+ relative motion. In contrast, for the smaller thermally hot clusters, where each atom initially possesses 1000 cm^{-1} of motional energy per degree of freedom, the solvent molecules appreciably populate regions of space near the NO_2^-:Li^+ interion axis (e.g., see Figure 7). It is therefore our speculation that energy transfer from the highly excited NO_2^-:Li^+ moiety to the surrounding solvent molecules is slow in the photodissociated case because the water molecules infrequently reside along the interion axis where impulsive interactions can occur. For the thermally hot clusters, the solvent molecules "roam" over larger regions, thereby more effectively interacting with NO_2^-:Li^+ and other solvent species.

b. Solvent Ejection Rates. Having discussed the resultant branching ratios for the two types of clusters, let us now turn our attention to the lifetimes for ejection of the water molecules. As stated above, we fit the decay profiles for the water molecules to single- or double-exponential functions as in eq 2 using a least-squares method. The parameters determined by this fit are listed in Tables III and IV for the thermally hot and photodissociated clusters, respectively. Recall that k_F^{-1} and k_S^{-1} (or equivalently $\tau_{F,S}$) are the fast and slow lifetimes, respectively, for the departing water molecules while A and B measure the fractions of the molecules which follow the fast or slow path.

The lifetimes for solvent loss shown in Tables III and IV range from a fraction of a picosecond to 30 ps. These rates are not dependent only upon the energy content of the cluster (recall that all clusters begin with 1000 cm^{-1} per degree of freedom); they are dependent upon the initial energy distribution. Consistent with the above observations relative to the loss of solvent in smaller clusters, we find slow decay rates for both the thermally hot and photodissociated $n = 1$ and $n = 2$ species. For the larger clusters, the rates of loss of the first solvent species are essentially identical (0.6 ps). As the daughter clusters become evaporatively cooled (covering a range of internal "temperatures" from 960 to 180 cm^{-1} per degree of freedom), the subsequent evaporation rates decrease. This is, of course, not surprising.

In the present study only short-time dynamics can be examined, it is simply impractical to extend our classical trajectories into even the microsecond regime. The computer expense would be prohibitive and numerical error in the trajectories could accumulate, thereby rendering the final results meaningless. Nevertheless, examination of the ~20-ps dynamics of these model prototype ion-pair clusters has shed light on the energetic and structural origins of their fragmentation branching ratios.

The ion-pair clusters studied in this work were intentionally designed to bridge the gap between small van der Waals clusters (e.g., ArHCl, H^-H_2O, or $Br_2^-CO_2$) where mode-specific behavior occurs and large clusters (e.g., $CO_2^+(CO_2)_{20}$, Ar_{30}^+, N_{42}^+) for which internal energy randomization is probably quite facile. Therefore, it is not surprising that we observed some behavior characteristic of both cluster classes.

V. Summary and Conclusions

In this paper, we report on the results of a molecular dynamics study of small NO_2^-:Li^+ hydrate clusters in which we performed two types of simulations. The first involved thermally hot clusters where all of the active degrees of freedom have the same amount (~1000 cm^{-1}) of energy initially. The second involved photodissociated clusters; here we equipartitioned a smaller amount (~300 cm^{-1} per degree of freedom) of energy among all of the active degrees of freedom and then we added an additional amount of energy to the NO_2^-:Li^+ interionic kinetic energy in order to simulate an impulsive dissociation of the ion pair.

In both studies we were interested in the transfer of energy among the cluster's degrees of freedom and the ultimate fate of this energy. For cluster sizes ranging from 1 to 5 water molecules, we determined lifetimes for the sequential loss of the solvent water molecules and branching ratios for production of the various daughter fragment clusters. We also examined the kinetic energy carried away by the ejected solvent molecules.

Our primary findings can be summarized as follows:

1. Although all clusters possessed enough internal energy to "boil off" all of their solvent molecules, kinetic energy carried away by the first solvent molecules ejected "cools" the resulting daughter clusters to an extent that loss of all solvent molecules does not occur.

2. The pattern of kinetic energy release is different for the photodissociated clusters than for the isoenergetic thermally hot clusters. This pattern, combined with the energy required to sequentially eject solvent molecules, determines the product-state branching ratios.

3. The ejected solvent molecules possess both translational and (often substantial) rotational kinetic energy.

4. For the $n = 5$ cluster, no dissociation to produce separately solvated ions is observed even though there is enough energy to do so. The sequential loss of solvent molecules is a more effective fragmentation channel.

5. For the smaller photodissociated clusters ($n = 1, 2$), inefficient energy transfer from the "hot" NO_2^-:Li^+ moiety to the H_2O solvent molecules is caused by the geometrical arrangement of the H_2O molecules relative to the NO_2^-:Li^+ interion axis. This slow energy transfer severely limits the rate of H_2O ejection. For the thermally hot clusters, in which the H_2O molecules possess enough motional energy to sample regions of space where energy transfer is favorable, such unusually slow H_2O ejection in $n = 1$ and $n = 2$ clusters is not seen.

6. The lifetimes for H_2O ejection in both the thermally hot and photodissociated clusters ranged from ~0.6 ps (for the first few water molecules in the larger clusters) to 10–30 ps for the "evaporatively cooled" daughter clusters and for very small ($n = 1, 2$) clusters.

7. For the $n = 4$ and $n = 5$ photodissociated clusters loss of the last *and* next-to-last H_2O molecules does not occur at any appreciable rate within 20 ps. Kinetic energy carried away by H_2O molecules ejected earlier cannot entirely explain this observation because at least as much kinetic energy is involved in the thermally hot cluster cases for which ejection of the next to last H_2O molecules *does* occur. Geometrical effects on the efficiency of energy transfer within the daughter clusters may again come into play.

There are significant implications of our findings for experimental work on gas-phase solvent-clustered ion pairs. First, it should be evident that measurements of the fragmentation branching ratios may provide probes both of energetics (kinetic energy release plus binding energies) and of geometry-imposed energy-transfer bottlenecks. It can also be predicted that, for clusters of the size studied here, the manner in which the total energy is initially deposited does affect the clusters fragmentation rates and branching ratios. Therefore, experiments which excite various chromophores in a given cluster seem called for.

Acknowledgment. The authors acknowledge the financial support of the U.S. Army Research Office (Grant No. DAAG-

2984K0086) and the Harris Corporation for their generous computer system grant.

Appendix

Newton's equations of motion were used to describe the translational degrees of freedom

$$\dot{\vec{r}}_i = \vec{v}_i \tag{A-1}$$

$$m\dot{\vec{v}}_i = \vec{F}_i = -\nabla_{\vec{r}_i}\sum_{j\neq i} V_{ij} \tag{A-2}$$

where $\vec{v}_i$ is the translational velocity of molecule i. The rotational degrees of freedom were described by Euler's equations of motion in the principal-axis frame of reference

$$I_i\frac{d\omega_i}{dt} + \epsilon_{ijk}\omega_j\omega_k I_k = N_i \tag{A-3}$$

where i here denotes the three spatial degrees of freedom.

The orientation of each molecule is usually specified by the Euler angles θ, ϕ, and Ψ. If we associate with a molecule a body-fixed coordinate system, then the Euler angles rotate the body-fixed system with respect to the space-fixed system.

The equations for the components of the angular velocity in terms of the Euler angles are (in the y convention)

$$\begin{pmatrix}\dot{\theta}\\ \dot{\phi}\\ \dot{\Psi}\end{pmatrix} = \begin{pmatrix}\sin\Psi & -\sin\theta\cos\Psi & 0\\ \cos\Phi & \sin\theta\sin\Psi & 0\\ 0 & \cos\theta & 1\end{pmatrix}^{-1}\begin{pmatrix}\omega_x\\ \omega_y\\ \omega_z\end{pmatrix} \tag{A-4}$$

$$\dot{\vec{\alpha}} = \Xi^{-1}\cdot\vec{\omega}_p \tag{A-5}$$

At $\theta = 0$ and π, Ξ is singular and the equations for the components of the angular velocity are unstable at these points. Hence, a set of angles with no singularities is desired. Such a set is known as quaternions which are described in terms of the Euler angles (in the y convention) as

$$e_0 = \chi = \cos\left(\frac{\Psi+\phi}{2}\right)\cos\frac{\theta}{2} \tag{A-6}$$

$$e_1 = \xi = \sin\left(\frac{\Psi-\phi}{2}\right)\sin\frac{\theta}{2} \tag{A-7}$$

$$e_2 = \eta = \cos\left(\frac{\Psi-\phi}{2}\right)\sin\frac{\theta}{2} \tag{A-8}$$

$$e_3 = \zeta = \sin\left(\frac{\Psi+\phi}{2}\right)\cos\frac{\theta}{2} \tag{A-9}$$

The equations for the components of the angular velocity can then be rewritten as

$$\begin{pmatrix}\omega_x\\ \omega_y\\ \omega_z\\ 0\end{pmatrix} = 2\begin{pmatrix}\chi & \zeta & -\eta & -\xi\\ -\zeta & \chi & \xi & -\eta\\ \eta & -\xi & \chi & -\zeta\\ \xi & \eta & \zeta & \chi\end{pmatrix}\begin{pmatrix}\dot{\xi}\\ \dot{\eta}\\ \dot{\zeta}\\ \dot{\chi}\end{pmatrix} \tag{A-10}$$

where $\chi^2 + \eta^2 + \xi^2 + \zeta^2 = 1$. In addition, the rotation matrix A can be written as ($V_{body} = \mathbf{A}\cdot V_{space}$)

$$\mathbf{A} = \begin{pmatrix}\chi^2+\xi^2-\eta^2-\zeta^2 & 2(\eta\xi+\chi\zeta) & 2(\xi\zeta-\chi\eta)\\ 2(\eta\xi-\chi\zeta) & \chi^2+\eta^2-\xi^2-\zeta^2 & 2(\eta\zeta+\chi\xi)\\ 2(\xi\zeta+\chi\eta) & 2(\eta\zeta-\chi\xi) & \chi^2-\xi^2-\eta^2+\zeta^2\end{pmatrix} \tag{A-11}$$

There are three advantages of the quaternions over the Euler angles. First, there are no singularities in the equations for the components of the angular velocity. Second, the matrix Ξ is now orthogonal. Third, no trigonometric function evaluations are needed.

The disadvantage is that the quaternions are not independent, but that does not present any numerical difficulties. Also, there are four variables instead of three as with Euler angles. This is not really a problem since the matrices in terms of quaternions are easier to calculate (no trigonometric calculations) and there are no singularities (allows a larger step size to be used), but it does add to the storage requirements.

Registry No. NO_2^-, 14797-55-8; Li^+, 17341-24-1; H_2O, 7732-18-5.

Collisional Effects in Organometallic Multiphoton Dissociation/Ionization Experiments: The Modeling of Townsend Discharges

Jeanne M. Hossenlopp and J. Chaiken*

Department of Chemistry, Syracuse University, Syracuse, New York 13244-1200
(Received: September 5, 1986; In Final Form: October 30, 1986)

We have measured the effects of added buffer gas on the multiphoton ionization (MPI) signal of various arene chromium tricarbonyls and $Cr(CO)_6$. Using basic gaseous electronics theory and experimental results on ion multiplication behavior in pure buffer gases, we have found the simplest method for quantitative analysis of collisional effects in MPI systems. We have applied this discharge model to the multiphoton ionization signal of chromium compounds as a function of helium, argon, and xenon pressures at a number of wavelengths and ion collection plate voltages. Where simple ion multiplication behavior holds, the measured ion signal is directly proportional to the initial MPI yield. This is of crucial importance for MPI studies where product branching ratios are being determined. When multiplication theory does not model the ion signal pressure dependence, other processes which may influence ion production in the system must be considered.

Introduction

We are interested in the unimolecular gas-phase photochemistry of organometallic molecules because of their possible utility in semiconductor fabrication, in preparing thin metal films[1] for various uses, and as photoactivated catalysts.[2] Multiphoton dissociation/ionization (MPD/MPI) spectroscopy has been utilized to study the photochemistry and photophysics of a variety of organometallics in both bulk gas[3-6] and molecular beam[7-10] ex-

(1) Mayer, T. M.; Fisanick, G. J.; Eichelberger IV, T. S.; *J. Appl. Phys.* **1982**, *53*, 8462.

(2) Schroeder, M. A.; Wrighton, M. S. *J. Am. Chem. Soc.* **1976**, *98*, 551.
(3) Engelking, P. C. *Chem. Phys. Lett.* **1980**, *74*, 207.

0022-3654/87/2091-2825$01.50/0